

Evaporation–Condensation Effects on Resonant Photoacoustics of Volatile Aerosols

RICHARD RASPET AND WILLIAM V. SLATON

National Center for Physical Acoustics, University of Mississippi, University, Mississippi

W. PATRICK ARNOTT AND HANS MOOSMÜLLER

Desert Research Institute, University of Nevada at Reno, Reno, Nevada

(Manuscript received 22 October 2001, in final form 30 October 2002)

ABSTRACT

In determining the optical properties of the atmosphere, the measurement of light absorption by aerosols is particularly challenging, and yet it is important because of the influence of strongly absorbing black carbon on climate and atmospheric visibility. The photoacoustic method obtains aerosol light absorption in situ, without use of filters, by acoustic measurement of the heat generated from aerosol light absorption, and its transfer to the surrounding air. However, in the general case, volatile aerosols heated by light absorption may also cool by evaporation (mass transfer). In this paper, the limiting case of the photoacoustic response of a volatile aerosol is compared with that of a dry aerosol to further the understanding of the data obtained with photoacoustic instruments. While the theory of photoacoustics of volatile aerosols for low-frequency, nonresonant cells has already been developed, current methods employ high-frequency, acoustically resonant photoacoustic instruments for quantifying atmospheric aerosol light absorption and vehicle exhaust mass concentration associated with black carbon. In this paper, a complete theory of photoacoustics for volatile aerosols is developed that includes additional terms to allow for higher-frequency devices, large particles, and high particle densities. Numerical calculations are used to determine the limits of various approximations.

1. Introduction

Incomplete combustion of carbonaceous fuels can result in the production of black carbon aerosol, with high emission rates per mass of fuel burned for small sources such as diesel engines and fireplaces (Horvath 1993). The optimal choices for fuel use and for methods of fuel combustion to generate energy continue to be developed and debated against a backdrop of societal concerns such as human health (e.g., Lighty et al. 2000), visibility (e.g., National Research Council 1993), and climate impacts (e.g., Andreae 2001). Black carbon aerosols strongly absorb light throughout much of the electromagnetic spectrum, with a characteristic dependence as inverse wavelength in the visible and near-IR. So, in addition to the potential health effects on breathing carbon aerosols, the impacts of light absorption on radiation transfer (e.g., Jacobson 2001), visibility (e.g., Horvath et al. 1983; Fox et al. 1999), and cloud dynamics (e.g., Ackerman et al. 2000; Hansen et al. 2000; Lohmann and Feichter 2001) are of concern.

Measurement of aerosol light absorption is difficult.

Direct measurements of aerosol extinction and scattering are often not accurate enough to obtain the often much smaller absorption by subtraction. Filter-based methods for the absorption measurement are simple, but suffer from lack of direct calibration methods, and from potential artifacts due to light scattering aerosol and relative humidity changes. Photoacoustic methods have been commonly applied to the detection and spectroscopy of trace gases in the atmosphere (Fiegel et al. 1989; Fiedler and Hess 1990; Miklos and Hess 2001; Sigrist 1994; Brand et al. 1995), and to a lesser extent, to the measurement of light absorption by aerosols (Bruce and Pinnick 1977; Terhune and Anderson 1977; Foot 1979; Truex and Anderson 1979; Faxvog and Roessler 1982; Roessler 1984; Adams et al. 1990a,b; Petzold and Niessner 1992, 1995; Moosmüller et al. 1998; Arnott et al. 1999, 2000; Moosmüller et al. 2001).

Photoacoustic signals are produced from the heat generated by light absorption (Rosencwaig 1980). In the case of aerosols, this heat is transferred to the surrounding air, generating an acoustic wave for a power-modulated light source. But, for aerosols, these signals may also be generated by mass transfer. For example, consider a small water droplet illuminated by a 6- μm wavelength laser. Water absorbs strongly at this wavelength and the droplet will absorb power from the laser beam

Corresponding author address: Dr. W. Patrick Arnott, Desert Research Institute, University of Nevada at Reno, 2215 Raggio Parkway, Reno, NV 89512.
E-mail: pat@dri.edu

in quantity equal to the droplet absorption cross section multiplied by the laser irradiance. Some of the absorbed laser power will heat the particle, and some will supply the latent heat necessary to add more water vapor molecules to the volume surrounding the droplet. These additional water vapor molecules contribute to the acoustic signal, in addition to the thermal expansion of the air as heat transfers from the droplet. But pure water droplets have a very low absorption cross section at visible wavelengths most relevant to the absorption of sunlight in the atmosphere. However black carbon aerosols (“soot”) do have strong absorption cross sections in the visible, and are responsible for most of the particulate light absorption in the atmosphere for visible wavelengths. Soot is known to uptake water vapor at relative humidities below 100%, with certain sites on the complex soot geometry (10–30-nm spherical monomers aggregated together to form particles of up to a few microns in maximum dimension) beginning to exhibit multilayer adsorption for relative humidity as low as 50% (Chughtai et al. 1999). The reduction of the photoacoustic signal by latent heat and mass transfer is analogous to the reduction observed in the photoacoustic spectrum of gaseous NO_2 when the light wavelength drops below 410 nm (Harshbarger and Robin 1973). In this case, 410 nm is the upper-wavelength threshold for photodissociation of NO_2 , so below this wavelength some of the radiant energy is used to break the bond between NO and O.

The analysis is tractable for the heat and mass transfer from heated water spheres; therefore, this problem will be used to gain insight on the effects of mass transfer to the photoacoustic signal. Though multilayer adsorption on soot is not likely to cover the entire soot surface even at 100% RH due to strong positive curvature on portions of the soot surface, and soot aerosols are certainly not spheres, it is argued that the spherical water droplet problem provides a useful insight for the effects of mass transfer on the photoacoustic signal. Dry soot particles can be modeled simply by setting the mass diffusion coefficient to zero in the theory, so that the entire photoacoustic signal is due to heat transfer. Then it will be demonstrated that the photoacoustic signal for a moist droplet is less than for a dry droplet, because of the energy expenditure in latent heat and the differences in the efficiency for sound generation from mass and heat injection to air. The theory is sufficiently general to encompass the previous approach for isolated aerosols in nonresonant photoacoustic instruments (Baker 1976) as well as a dense cloud of aerosols in more commonly used resonant photoacoustic cells (Adams et al. 1990a; Petzold and Niessner 1995; Arnott et al. 1999, 2000). The analysis is based on the low reduced frequency method used previously to evaluate the effects of evaporation–condensation on sound propagation in wet walled tubes (Raspet et al. 1999; Hickey et al. 2000).

It should be noted that while our chief concern is

measurement of light absorption by soot as it is influenced by water vapor, the theory developed below is formally complete for understanding photoacoustic signals from pure liquid droplets. One major objective of the paper is to arrive at the ratio of the photoacoustic signals for wet and “dry” droplets (droplets are dried, in theory, simply by setting the mass diffusion coefficient to zero.) This ratio should provide a reasonable first estimate for the effect of high RH (very near 100%) on photoacoustic signals from presumably hygroscopic carbon aerosols. This ratio does not depend on the absorption cross section of the droplet, when in the linear optics regime, as the heat and mass transfer are both driven linearly by the optical power absorbed by the particle. More work, beyond the scope of this paper, is necessary to develop a full model for photoacoustic signals at visible wavelengths from cloud droplets with embedded black carbon aerosol, and for mass transfer from water vapor adsorbed on black carbon aerosol at $\text{RH} < 100\%$.

2. Theory

Photoacoustic instruments usually are designed to measure light absorption in a flow-through acoustic resonator. The laser beam cross-sectional area is much smaller than the area of this resonator. We therefore assume that the residence time of the particles in the beam is small compared with the time for significant DC mass evaporation to occur. The laser excitation can be considered as a DC component producing steady evaporation and heating and an AC component that will alternately heat and cool the particle. Our analysis will concentrate on the AC component. In addition, we assume that each particle of radius r_0 is surrounded by similar neighbors and that each droplet exchanges heat and vapor with its neighborhood of radius $a = 1/N^{1/3}$ where N is the aerosol particle density in m^{-3} .

The governing equations are the Navier–Stokes equation, the continuity equation for each component and for the mixture, the entropy equation for the mixture, the equation of state for the mixture, and the diffusion equation for the mixture. In linearized form these are (Landau and Lifshitz 1997; Hirschfelder et al. 1954)

$$\rho_0 \frac{\partial \mathbf{v}}{\partial t} = -\nabla p + \mu \nabla^2 \mathbf{v} + \left(\beta + \frac{1}{3} \mu \right) \nabla (\nabla \cdot \mathbf{v}), \quad (1)$$

$$\frac{\partial \rho_1}{\partial t} + \rho_1^0 (\nabla \cdot \mathbf{v}_1) = 0, \quad (2a)$$

$$\frac{\partial \rho_2}{\partial t} + \rho_2^0 (\nabla \cdot \mathbf{v}_2) = 0, \quad (2b)$$

$$\frac{\partial \rho}{\partial t} + \rho_0 (\nabla \cdot \mathbf{v}) = 0, \quad (2c)$$

$$\begin{aligned} -\frac{\partial p}{\partial t} + \frac{\gamma}{\gamma-1}nk\frac{\partial T}{\partial t} - \kappa\nabla^2 T + k_TnkT\nabla \cdot (\mathbf{v}_1 - \mathbf{v}_2) \\ = 0, \end{aligned} \quad (3)$$

$$\frac{\partial p}{\partial t} = nk\frac{\partial T}{\partial t} + kT_0\left(\frac{1}{m_1}\frac{\partial \rho_1}{\partial t} + \frac{1}{m_2}\frac{\partial \rho_2}{\partial t}\right), \quad \text{and} \quad (4)$$

$$\begin{aligned} \mathbf{v}_1 - \mathbf{v}_2 = D_{12}\left(\frac{1}{\rho_2^0}\nabla\rho_2 - \frac{1}{\rho_1^0}\nabla\rho_1 - \frac{n}{\rho_0 P_0}(m_2 - m_1)\nabla p \right. \\ \left. - \frac{n^2}{n_1 n_2} \cdot \frac{k_T}{T_0}\nabla T\right). \end{aligned} \quad (5)$$

In these equations, variables ρ_1 , ρ_2 are the density of the gas and of the vapor; $\rho = \rho_1 + \rho_2$ is the density of the mixture; \mathbf{v}_1 , \mathbf{v}_2 are the hydrodynamic velocity of the gas and of the vapor; $\mathbf{v} = (\rho_1\mathbf{v}_1 + \rho_2\mathbf{v}_2)/\rho$ is the hydrodynamic velocity of the mixture; p is the pressure of the mixture; and T is the temperature of the mixture. In the above equations, μ is the viscosity of the mixture; β is the bulk viscosity of the mixture; m_1 , m_2 are the molecular mass of gas and vapor; n_1 , n_2 are the number densities of the gas and of the vapor; $n = n_1 + n_2$ is the total number density; γ_1 , γ_2 are the ratio of specific heats of the gas and of the vapor; $n\gamma/(\gamma-1) = n_1\gamma_1/(\gamma_1-1) + n_2\gamma_2/(\gamma_2-1)$ is the ratio of nc_p/R for the mixture; c_p is the molar heat capacity at constant pressure; R is the universal gas constant; κ is the thermal conductivity of the mixture; D_{12} is the mass diffusion coefficient; k_T is the thermal diffusion ratio as defined in Hirshfelder et al. (1954, p. 541); k is Boltzmann's constant; and the subscript/superscripts 0 refer to ambient values of quantities. The bulk viscosity accounts for the small departure of the rotational and translational modes from thermodynamic equilibrium.

The linearized heat equation for the particle is given by

$$\frac{\partial}{\partial t}(\rho_p c_{pp} T_p) - \kappa_p \nabla^2 T_p = L(t). \quad (6)$$

Here, ρ_p is the particle density, c_{pp} is the particle heat capacity at constant pressure, κ_p is the particle heat conductivity, T_p the temperature of the particle, and $L(t)$ is the laser power absorbed by the particle per unit volume. Assuming single frequency excitation we set $L(t) = L_0 e^{-i\omega t}$, where $L_0 = \alpha I_0$, I_0 is the magnitude of the laser beam intensity at the operating frequency, and α (dimensions of inverse distance) is the absorption cross section of the particle divided by its volume. We assume that the absorbed energy is distributed uniformly through the particle much faster than the inverse acoustic frequency, so that the particle is evenly heated. We assume also that the resulting diffusion and heat flow will be predominately radial and define two dimensionless variables,

$$\eta = \frac{r}{a}, \quad (7)$$

the dimensionless radius, and the reduced frequency,

$$\Omega = \frac{\omega a}{c}. \quad (8)$$

Assuming that all the variables have an $e^{-i\omega t}$ time dependence where ω is the angular frequency of the modulated laser beam, we introduce normalized variables as follows:

$$p = \frac{\rho_0 c^2}{\gamma}(1.0 + p^* e^{-i\omega t}), \quad (9a)$$

$$T = T_0(1.0 + T^* e^{-i\omega t}), \quad (9b)$$

$$T_p = T_0(1 + T_p^* e^{-i\omega t}), \quad (9c)$$

$$\mathbf{v} = c\mathbf{v}^* e^{-i\omega t}, \quad \text{and} \quad (9d)$$

$$\mathbf{v}_1 - \mathbf{v}_2 = c\mathbf{V}^* e^{-i\omega t}, \quad (9e)$$

where c is the sound speed in the mixture and asterisks denote normalized values. The normalization assures that all variables are of the same order.

Using the definitions above, the Navier–Stokes equation becomes

$$\frac{1}{\gamma} \frac{\partial p^*}{\partial \eta} - i\Omega \mathbf{v}^* - \frac{\Omega}{\lambda_\mu^2} \frac{\partial}{\partial \eta} \left[\frac{1}{\eta^2} \frac{\partial(\eta^2 \mathbf{v}^*)}{\partial \eta} \right] = 0. \quad (10)$$

where $\lambda_\mu = a\sqrt{\omega\rho/(\beta + (4/3)\mu)}$. Note that this definition of the dimensionless viscous wave number is not the same as the shear wavenumber defined in (Raspet et al. 1999). The entropy equation is given by

$$\begin{aligned} \Omega \frac{\gamma-1}{\gamma} p^* - \Omega T^* + i \frac{\Omega}{\lambda_T^2} \frac{1}{\eta^2} \frac{\partial}{\partial \eta} \left(\eta^2 \frac{\partial T^*}{\partial \eta} \right) \\ - i \frac{\gamma-1}{\gamma} \frac{k_T}{\eta^2} \frac{\partial(\eta^2 V^*)}{\partial \eta} = 0, \end{aligned} \quad (11)$$

where $\lambda_T = a\sqrt{\rho\omega c_p/\kappa}$, is the dimensionless thermal wavenumber. We note that λ_T may be written in terms of the thermal penetration depth δ_T as $\lambda_T = \sqrt{2}a/\delta_T$. The equation of state is combined with the continuity equations of each component to form the equation of state in terms of p^* , T^* , \mathbf{v}^* , and V^* :

$$\begin{aligned} \Omega p^* - \Omega T^* + \frac{i}{\eta^2} \frac{\partial(\eta^2 \mathbf{v}^*)}{\partial \eta} \\ - i \frac{n_1 n_2}{n \rho_0} (m_1 - m_2) \frac{1}{\eta^2} \frac{\partial(\eta^2 V^*)}{\partial \eta} = 0. \end{aligned} \quad (12)$$

The final equation results from combining the diffusion equation with the continuity relations,

$$V^* - \frac{i}{\lambda_D^2} \frac{\partial}{\partial \eta} \left[\frac{1}{\eta^2} \frac{\partial(\eta^2 V^*)}{\partial \eta} \right] - \frac{\Omega}{\lambda_D^2} \left[\frac{n}{\rho_0} (m_1 - m_2) \frac{\partial p^*}{\partial \eta} - \frac{n^2 k_T}{n_1 n_2} \frac{\partial T^*}{\partial \eta} \right] = 0, \quad (13)$$

where $\lambda_D = a\sqrt{\omega/D_{12}}$ is the dimensionless diffusion wave number. The temperature equation in the particle is

$$T_p^* - \frac{i}{\lambda_p^2} \frac{1}{\eta^2} \frac{\partial}{\partial \eta} \left(\eta^2 \frac{\partial T_p^*}{\partial \eta} \right) = \frac{iL_0}{c_{pP} \rho_p \omega T_0}, \quad (14)$$

where $\lambda_p = a\sqrt{\rho_p \omega c_{pP} / \kappa_p}$ is the dimensionless thermal wave number in the particle. Note that this is defined with respect to the neighborhood radius a , not with respect to the particle radius r_0 .

Next p^* and $\partial p^* / \partial \eta$ are eliminated from Eqs. (10)–(13) to form three differential equations in v^* , V^* , and T^* . The first equation is formed by eliminating the common pressure term between Eqs. (11) and (12). The second equation comes from removing the common pressure partial derivative term between Eqs. (10) and (13). Finally, the third equation is obtained by taking the partial derivative of Eq. (12), and removing the common pressure derivative term between it and Eq. (13). The low reduced-frequency approximation is applied to the three equations: all terms containing Ω^2 are dropped because the interparticle spacing is much less than the acoustic wavelength, and Ω is small, even for low number densities and high operating frequencies. ($\Omega \approx 0.04$ for $N = 350$ particles cm^{-3} and $f = 2000$ Hz.) The v^* term is eliminated from the three equations to form two coupled equations in V^* and T^* :

$$\frac{\partial T^*}{\partial \eta} - \frac{i}{\lambda_T^2} \frac{\partial}{\partial \eta} \left[\frac{1}{\eta^2} \frac{\partial}{\partial \eta} \left(\eta^2 \frac{\partial T^*}{\partial \eta} \right) \right] + i \frac{\gamma - 1}{\gamma} \frac{k_T}{\Omega} \frac{\partial}{\partial \eta} \left[\frac{1}{\eta^2} \frac{\partial(\eta^2 V^*)}{\partial \eta} \right] = 0, \quad (15)$$

and

$$\frac{\Omega}{\lambda_D^2} \frac{n^2 k_T}{n_1 n_2} \frac{\partial T^*}{\partial \eta} + \left\{ V^* - \frac{i}{\lambda_D^2} \frac{\partial}{\partial \eta} \left[\frac{1}{\eta^2} \frac{\partial(\eta^2 V^*)}{\partial \eta} \right] \right\} = 0. \quad (16)$$

The coupling between the temperature fluctuations and diffusion fluctuations in the mixture is provided by the terms containing the thermal diffusion ratio k_T , which appears in the entropy equation due to diffusion across the control volume and in the diffusion equation from temperature driven diffusion. These variables are coupled by the boundary conditions at the particle surface as described below.

These equations, combined with boundary conditions and the temperature equation in the particle represent a complete solution. The solution of the coupled equations lead to two modes of propagation. An investigation of the effect of the k_T coupling shows it to cause a neg-

ligible change in the wavenumbers for thermal and mass diffusion fluctuations (Hickey et al. 2000). In the remainder of the paper, k_T is set to zero. For photoacoustics in the atmosphere, the mole fraction of vapor will be very low (less than 0.05) and the effect of the coupling of the diffusion and thermal wavenumbers low. In (Hickey et al. 2000) the calculated fractional change in thermal and diffusive wave numbers for water vapor in air is less than 10^{-4} for temperatures up to 30°C . The use of the low reduced-frequency approximation and the modal analysis of Hickey et al. (2000) demonstrates that Baker's use of simplified hydrodynamic equations is justified for the present analysis of higher frequency devices. The boundary conditions for the solution of this problem are developed within these approximations. Diffusion and thermal effects are assumed to dominate the acoustic terms in the particle neighborhood.

3. Boundary conditions

The boundary conditions at the neighborhood boundary ($r = a$) are

$$V^*|_{\eta=1} = 0, \quad \text{and} \quad (17a)$$

$$\left. \frac{\partial T^*}{\partial \eta} \right|_{\eta=1} = 0. \quad (17b)$$

At the particle radius, r_0 , the inert gas velocity must be zero, the temperature must be continuous, the heat generated by condensation at the surface must be carried away by the heat flux into the gas and particle, and the diffusion velocity can be calculated from the temperature at the particle radius. We require that the temperature in the particle, T_p^* , and the gas mixture, T^* , be equal at the particle radius ($\eta = r_0/a$):

$$T^*|_{\eta=r_0/a} = T_p^*|_{\eta=r_0/a}. \quad (18)$$

Next, we require heat flux balance at the particle radius. In general, this can be written as

$$\mathbf{q} = \kappa_p \nabla T_p - \kappa \nabla T, \quad (19)$$

where \mathbf{q} is the heat flux generated at the boundary. For a liquid particle the heat flux generated may be written, $\mathbf{q} = l \mathbf{m}_{\text{flux}} = -l \rho_2^0 \mathbf{v}_2(r_0/a)$, where ρ_2^0 is the ambient vapor density, $\mathbf{v}_2(r_0/a)$ is the average radial velocity of the vapor evaluated at the particle surface, and l is the latent heat of vaporization. Thus, our boundary condition for the heat flux at $\eta = r_0/a$ becomes

$$-l \rho_2^0 \mathbf{v}_2 = \kappa_p \nabla T_p - \kappa \nabla T. \quad (20)$$

Use of the normalization definitions in Eqs. (9a)–(9e), and the fact that $v_1 = 0$ at the particle surface, yields the following equation for the heat flux:

$$-l \rho_2^0 \frac{cV^*}{T_0} \bigg|_{\eta=r_0/a} = \left[\frac{\kappa}{a} \frac{\partial T^*}{\partial \eta} - \frac{\kappa_p}{a} \frac{\partial T_p^*}{\partial \eta} \right]_{\eta=r_0/a}. \quad (21)$$

Temperature fluctuations at the particle surface induce

vapor pressure fluctuations. The Clausius–Clapeyron equation (Reif 1965),

$$p_{\text{vapor}}|_{\eta=r_0/a} = p_0 \exp\left[-\frac{lm_2}{R}\left(\frac{1}{T} - \frac{1}{T_{\text{REF}}}\right)\right]_{\eta=r_0/a}, \quad (22)$$

relates the vapor pressure to the temperature. A linearized expression for the density of the vapor near the particle can be derived from the ideal gas law and Eq. (22):

$$\rho_2|_{\eta=r_0/a} = \rho_2^0 \left[1 + \left(\frac{lm_2}{RT_0} - 1\right)T^*e^{-i\omega t}\right]_{\eta=r_0/a}, \quad (23)$$

where T_0 is the ambient temperature of the system. The equation of continuity can then be used to write Eq. (23) in terms of V^* and T^* :

$$i\frac{1}{\eta^2}\frac{\partial}{\partial\eta}(\eta^2V^*)|_{\eta=r_0/a} = \Omega\frac{\rho_0}{\rho_1^0}\left(\frac{lm_2}{RT_0} - 1\right)T^*|_{\eta=r_0/a}. \quad (24)$$

The divergence of v^* is dropped from this boundary condition as v^* at the boundary is smaller than V^* by the ratio ρ_2/ρ and v^* is principally an acoustic wave with small spatial variation compared to diffusion and heat conduction (Pierce 1989, 519–531). The fourth boundary condition is that the time rate of heat flow out of the particle at r_0 must equal the time rate of change in internal energy in the particle neighborhood,

$$4\pi r_0^2\frac{\kappa}{a}\frac{\partial T^*}{\partial\eta}\bigg|_{\eta=r_0/a} = -i\omega\int_{\eta=r_0/a}^{\eta=1}\rho c_p T^*(\eta)4\pi a^3\eta^2 d\eta. \quad (25)$$

Again, this boundary condition is only correct if the acoustic energy is negligible with respect to the internal energy.

4. Solution

The set of differential equations to be solved are

$$\frac{\partial T^*}{\partial\eta} - \frac{i}{\lambda_T^2}\frac{\partial}{\partial\eta}\left[\frac{1}{\eta^2}\frac{\partial}{\partial\eta}\left(\eta^2\frac{\partial T^*}{\partial\eta}\right)\right] = 0, \quad (26)$$

$$V^* - \frac{i}{\lambda_D^2}\frac{\partial}{\partial\eta}\left[\frac{1}{\eta^2}\frac{\partial(\eta^2V^*)}{\partial\eta}\right] = 0, \quad \text{and} \quad (27)$$

$$T_p^* - \frac{i}{\lambda_p^2}\frac{1}{\eta^2}\frac{\partial}{\partial\eta}\left(\eta^2\frac{\partial T_p^*}{\partial\eta}\right) = \frac{iL_0}{c_{pP}\rho_P\omega T_0}. \quad (28)$$

These are respectively Eqs. (15) and (16) with $k_T = 0$, and Eq. (14) repeated for completeness. The solutions are in terms of spherical Bessel and Hankel functions. We choose solutions so that T_p^* is finite at $r = 0$ and so that $\partial T^*/\partial\eta$ and V^* are zero at $r = a$. The solutions are

$$\frac{\partial T^*}{\partial\eta} = Af_1(\lambda_T\eta, \lambda_T), \quad (29)$$

$$V^* = Bf_1(\lambda_D\eta, \lambda_D), \quad \text{and} \quad (30)$$

$$T_p^* = Dj_0(\sqrt{i}\lambda_p\eta) + i\frac{L_0}{c_{pP}\rho_P\omega T_0}. \quad (31)$$

where A , B , and D are constants to be determined from the boundary conditions, and $f_1(\lambda\eta, \lambda)$ and $f_0(\lambda\eta, \lambda)$ are defined as

$$f_1(\lambda\eta, \lambda) = -\lambda^2\eta_0^2\left[h_1^{(1)}(\sqrt{i}\lambda\eta) - h_1^{(2)}(\sqrt{i}\lambda\eta)\frac{h_1^{(1)}(\sqrt{i}\lambda)}{h_1^{(2)}(\sqrt{i}\lambda)}\right], \quad (32)$$

and

$$f_0(\lambda\eta, \lambda) = i\sqrt{i}\lambda\eta_0\left[h_0^{(1)}(\sqrt{i}\lambda\eta) - h_0^{(2)}(\sqrt{i}\lambda\eta)\frac{h_1^{(1)}(\sqrt{i}\lambda)}{h_1^{(2)}(\sqrt{i}\lambda)}\right], \quad (33)$$

where $\eta_0 = r_0/a$. The functions f_1 and f_0 are chosen so that they approach one for the small particle, large neighborhood limit. This facilitates comparison with Baker’s (1976) theory. Recursion relations for the spherical Bessel functions give

$$\frac{1}{\eta^2}\frac{\partial}{\partial\eta}[\eta^2f_1(\lambda\eta, \lambda)] = i\lambda^2\eta_0f_0(\lambda\eta, \lambda), \quad (34)$$

$$\frac{\partial}{\partial\eta}[f_0(\lambda\eta, \lambda)] = -\frac{f_1(\lambda\eta, \lambda)}{\eta_0}, \quad \text{and} \quad (35)$$

$$\frac{\partial}{\partial\eta}\left\{\frac{1}{\eta^2}\frac{\partial}{\partial\eta}[\eta^2f_1(\lambda\eta, \lambda)]\right\} = -i\lambda^2f_1(\lambda\eta, \lambda). \quad (36)$$

Integration of Eq. (26) gives

$$T^*(\eta) = -\eta_0Af_0(\lambda_T\eta, \lambda_T) + C, \quad (37)$$

where C is an integration constant. Substitution of this form in Eq. (25) shows that C is identically zero. The temperature matching boundary condition, Eq. (18), becomes

$$Dj_0(\sqrt{i}\lambda_p\eta_0) + \frac{iL_0}{c_{pP}\rho_P\omega T_0} = -\eta_0Af_0(\lambda_T\eta_0, \lambda_T). \quad (38)$$

The heat flux boundary condition, Eq. (21), is given by

$$\begin{aligned} & -\frac{l\rho_2^0c}{T_0}Bf_1(\lambda_D\eta_0, \lambda_D) \\ & = \frac{\kappa}{a}Af_1(\lambda_T\eta_0, \lambda_T) + \frac{\kappa_P}{a}\sqrt{i}\lambda_P Dj_1(\sqrt{i}\lambda_P\eta_0). \end{aligned} \quad (39)$$

The boundary condition that expresses the vapor pressure in terms of the surface temperature of the particle gives

$$\begin{aligned} & \lambda_D^2 \eta_0 B f_0(\lambda_D \eta_0, \lambda_D) \\ &= \Omega \frac{\rho_0}{\rho_1^0} \left(\frac{lm_2}{RT_0} - 1 \right) \eta_0 A f_0(\lambda_T \eta_0, \lambda_T). \end{aligned} \quad (40)$$

Eliminating D from Eqs. (38) and (39), we find

$$\begin{aligned} & \frac{\kappa}{a} A f_1(\lambda_T \eta_0, \lambda_T) + \frac{l \rho_2^0 c}{T_0} B f_1(\lambda_D \eta_0, \lambda_D) \\ &= \sqrt{i} \lambda_p \frac{\kappa_p j_1(\sqrt{i} \lambda_p \eta_0)}{a j_0(\sqrt{i} \lambda_p \eta_0)} \\ & \quad \times \left[\frac{i Q_0}{c_{pp} \rho_p \omega T_0} + \eta_0 A f_0(\lambda_T \eta_0, \lambda_T) \right]. \end{aligned} \quad (41)$$

The product $\lambda_p \eta_0$ is usually small; small argument expansions can be used to express Eq. (41) in simpler form.

Let $c' = (3/\sqrt{i} \lambda_p \eta_0) [j_1(\sqrt{i} \lambda_p \eta_0)/j_0(\sqrt{i} \lambda_p \eta_0)] \cong 1 + i/15(\lambda_p \eta_0)^2$. This normalization also facilitates comparison with Baker (1976). Baker assumes that taking $c' = 1$ is sufficient. Gathering terms we find

$$\begin{aligned} & \frac{\kappa}{a} A f_1(\lambda_T \eta_0, \lambda_T) \left[1 - i \frac{c_{pp} \rho_p \omega r_0^2 c'}{3\kappa} \frac{f_0(\lambda_T \eta_0, \lambda_T)}{f_1(\lambda_T \eta_0, \lambda_T)} \right] \\ &+ \frac{l \rho_2^0 c}{T_0} B f_1(\lambda_D \eta_0, \lambda_D) = -\frac{L_0 c' r_0}{3T_0}. \end{aligned} \quad (42)$$

From Eq. (40),

$$B = \left[\frac{D_{12} \rho_0}{ac \rho_1^0} \left(\frac{lm_2}{RT_0} - 1 \right) \frac{f_0(\lambda_T \eta_0, \lambda_T)}{f_0(\lambda_D \eta_0, \lambda_D)} \right] A. \quad (43)$$

Equation (42) is solved for A :

$$A = -\frac{L_0 c' r_0 a}{3\kappa T_0 f_1(\lambda_T \eta_0, \lambda_T) \Xi}, \quad (44)$$

where

$$\Xi = 1 - iTh + lEv, \quad (45a)$$

$$Th = \frac{c_{pp} \rho_p \omega r_0^2 c'}{3\kappa} \frac{f_0(\lambda_T \eta_0, \lambda_T)}{f_1(\lambda_T \eta_0, \lambda_T)}, \quad \text{and} \quad (45b)$$

$$\begin{aligned} Ev &= \frac{\rho_2^0 D_{12} \rho_0}{\kappa T_0 \rho_1^0} \left(\frac{lm_2}{RT_0} - 1 \right) \\ & \quad \times \frac{f_0(\lambda_T \eta_0, \lambda_T) f_1(\lambda_D \eta_0, \lambda_D)}{f_1(\lambda_T \eta_0, \lambda_T) f_0(\lambda_D \eta_0, \lambda_D)}. \end{aligned} \quad (45c)$$

The constants A and B may be combined with Eqs. (29) and (30) to evaluate $\partial T^*/\partial \eta$ and V^* . For the present investigation of photoacoustics, we evaluate the acoustic source terms rather than the variables $\partial T^*/\partial \eta$ and V^* . The wave equation with mass and heat injection is given in (Morse and Ingard 1986, 322–325), and is here translated to the frequency domain as

$$\nabla^2 P + \frac{\omega^2}{c^2} P = -f(\mathbf{r}, \omega), \quad (46)$$

where,

$$f(\mathbf{r}, \omega) = -i\omega \left(M + \frac{\gamma - 1}{c^2} H \right). \quad (47)$$

Here, M is the rate of mass injection per unit volume and H is the power added per unit volume due to heat transfer. The mass injection rate per unit volume is calculated by the product of $\rho_2 v_2$ at the particle surface times the surface area divided by the neighborhood volume:

$$\begin{aligned} M &= \left(\frac{r_0}{a} \right)^3 \frac{L_0 c' \rho_2^0 D_{12} \rho_0}{\kappa T_0 \Xi} \frac{\rho_0}{\rho_1^0} \left(\frac{lm_2}{RT_0} - 1 \right) \\ & \quad \times \frac{f_0(\lambda_T \eta_0, \lambda_T) f_1(\lambda_D \eta_0, \lambda_D)}{f_1(\lambda_T \eta_0, \lambda_T) f_0(\lambda_D \eta_0, \lambda_D)} \\ &= c' \left(\frac{r_0}{a} \right)^3 \frac{L_0 Ev}{\Xi} \equiv m \left(\frac{r_0}{a} \right)^3 L_0. \end{aligned} \quad (48)$$

The thermal power per unit volume is determined by summing the thermal flux over the surface divided by the neighborhood volume:

$$H = \left(\frac{r_0}{a} \right)^3 \frac{L_0 c'}{\Xi} \equiv h \left(\frac{r_0}{a} \right)^3 L_0. \quad (49)$$

By these definitions, m and h are the ratios of the rate of change of mass and thermal energy emission to the laser power absorption.

For N absorbing droplets per unit volume, of volume V_0 , with absorption cross section per particle volume α , the absorption coefficient is given by $B_{\text{abs}} = \alpha N V_0 = \alpha (r_0/a)^3$. Then the laser power absorbed per particle volume is given by $L_0 = B_{\text{abs}} I_0 / N V_0 = (a/r_0)^3 B_{\text{abs}} I_0$, where $I_0(x, \omega)$ is the magnitude of the laser intensity as a function of position and frequency. With this notation,

$$f(\mathbf{r}, \omega) = -i\omega \left\{ \left(m + \frac{\gamma - 1}{c^2} h \right) B_{\text{abs}} I_0(x, \omega) \right\}. \quad (50)$$

This last expression is a general form for the photoacoustic source term to drive the wave equation for pressure, Eq. (46), when aerosols can transfer both heat and mass.

To gain insight on a contemporary instrument (Arnott et al. 2000) used for measurement of light absorption by aerosols, Eq. (50) can be used as the source term for this 1D plane wave resonator. This resonator is bent at pressure nodes to facilitate laser beam and sample air passage through holes placed at the nodes (Arnott et al. 1999). When operated at acoustic resonance, the photoacoustic response from droplets in this resonator is given by

$$\frac{P_{\text{mic}}(f_{\text{res}})}{P_{\text{laser}}(f_{\text{res}})} = \frac{Q}{\pi^2 f_{\text{res}} A_{\text{res}}} [mc^2 + (\gamma - 1)h] B_{\text{abs}}. \quad (51)$$

Here, $P_{\text{laser}}(f_{\text{res}})$ is the laser power at resonance frequency f_{res} , Q is the quality factor of the resonator, A_{res} is the cross-sectional area of the resonator, and $P_{\text{mic}}(f_{\text{res}})$ is the acoustic pressure measured at the end of the resonator. Setting $m = 0$ and $\Xi = 1$ in Eq. (49) recovers the results of (Arnott et al. 1999, 2000) where only heat transfer is included.

5. Analysis

The results derived above are valid for general acoustic frequencies, particle sizes, and particle number densities (neighborhood radii). This complete analysis insures that the theory will correctly describe possible future devices exploring higher frequencies or multiple frequencies to investigate the effect of volatile components on photoacoustics. In this section, we will examine the differences between Baker's (1976) low-frequency, isolated particle result and our result, and we will evaluate the limiting case for the effects of water saturation on photoacoustic measurements of aerosol light absorption.

The low reduced-frequency solution results in functions of reduced radius η and dimensionless wave numbers λ . For the analysis of validity it is more intuitive to express these factors in terms of the ratio of the particle radius or neighborhood radius to the thermal or diffusive penetration depth in the particle or gas. The penetration depths can be interpreted as the distance heat (or mass) can diffuse during one acoustic period. The definitions of the thermal and diffusive penetration depths were given earlier. With those definitions the dimensionless wave numbers can be written as $\lambda_T = \sqrt{2}a/\delta_T$; $\lambda_D = \sqrt{2}a/\delta_D$ and $\lambda_T \eta_0 = \sqrt{2}r_0/\delta_T$; $\lambda_D \eta_0 = \sqrt{2}r_0/\delta_D$. The penetration depths are functions of temperature but near 20°C at 1500 Hz $\delta_{T_{\text{water}}} \approx 18 \mu\text{m}$, $\delta_{T_{\text{air}}} \approx 64 \mu\text{m}$ and $\delta_{D_{\text{air}}} \approx 69 \mu\text{m}$. These may be scaled to other frequencies by multiplication by $(1500/f)^{1/2}$. For example, at Baker's (1976) assumed frequency of 20 Hz, $\delta_{T_{\text{water}}}$ is about 160 μm .

Equations (48), (49), and (45a,b) have been written to facilitate comparison with Baker's low-frequency, small particle, large spacing results. Baker's results are recovered by setting,

$$c' = 1, \quad (52)$$

$$\frac{f_0(\lambda_T \eta_0, \lambda_T) f_1(\lambda_D \eta_0, \lambda_D)}{f_1(\lambda_T \eta_0, \lambda_T) f_0(\lambda_D \eta_0, \lambda_D)} = 1, \quad \text{and} \quad (53)$$

$$\text{Th} = \frac{c_{pP} \rho_P \omega r_0^2 c'}{3\kappa} \frac{f_0(\lambda_T \eta_0, \lambda_T)}{f_1(\lambda_T \eta_0, \lambda_T)} = 0. \quad (54)$$

In the following we will discuss the limits of validity of each term and establish useful approximations.

a. Effect of particle size on the temperature profile in the particle, $c' = 1$

The limits on this condition are best expressed by examining the second term in the expansion of the ratio of j_1 to j_0 in terms of the thermal penetration depth in the particle,

$$c' \cong 1 + \frac{i}{15} \left(\sqrt{2} \frac{r_0}{\delta_{T_p}} \right)^2 \cong 1 + 0.13i \left(\frac{r_0}{\delta_{T_p}} \right)^2. \quad (55)$$

For a particle size of one penetration depth, the magnitude of c' will differ from one by about 1% with a phase change of 0.13 radians. The second term in c' will be necessary for droplets larger than 18 μm at 1500 Hz and larger than 5 μm at 20 kHz. At 1500 Hz $c' = 1$ is a valid assumption for most atmospheric aerosols; at higher frequencies the second term should be included. In fact, for cases where c' is not unity, one must also consider the spatial distribution of absorbed radiant energy within the particle. The theoretical problem becomes much more complex in this case, as the kinetics of mass transfer become involved, and is beyond the scope of the present analysis.

b. Effect of finite neighborhoods on $f_0(\lambda \eta_0, \lambda)/f_1(\lambda \eta_0, \lambda)$

Figure 1 displays the magnitude of the ratio of functions versus the normalized particle radius and normalized neighborhood thickness $[(a - r_0)/\delta_T]$. The ratio of $f_0(\lambda \eta_0, \lambda)/f_1(\lambda \eta_0, \lambda)$ varies significantly from unity for small neighborhood thickness and for large particle radii. No significant correction for finite neighborhood radii is required for $a \geq \delta_T$. For small particles ($r_0/\delta_T < 10^{-2}$), neighborhood thickness as small as 0.3 δ_T may be neglected. For the Desert Research Institute (DRI) instrument operated in air at 1500 Hz, $\delta_{T_{\text{air}}} \approx 64 \mu\text{m}$. This corresponds to a particle number density of 10^6 particles cm^{-3} . At 20 Hz, the critical particle number density is about 1.5×10^3 particles cm^{-3} . The particle number densities for the 1500-Hz instrument are unlikely to occur in natural aerosols, but may be exceeded in studies of undiluted exhausts. The higher-frequency instruments are useful for higher particle densities because the penetration depths are small for them.

The ratio $f_0(\lambda \eta_0, \lambda)/f_1(\lambda \eta_0, \lambda)$ displays a dependence on particle radius, even when the neighborhood radius can be taken as infinite. This dependence can be greatly simplified by dropping the second term in the definitions of f_1 and f_0 and substituting the spherical Hankel functions $h_0^1(\lambda \eta_0)$ and $h_1^1(\lambda \eta_0)$:

$$\begin{aligned} \frac{f_0(\lambda \eta_0, \lambda)}{f_1(\lambda \eta_0, \lambda)} &= \frac{1}{1 - i\sqrt{i}\lambda \eta_0} \\ &= \frac{1}{(1 + r_0/\delta) - i(r_0/\delta)}, \end{aligned} \quad (56)$$

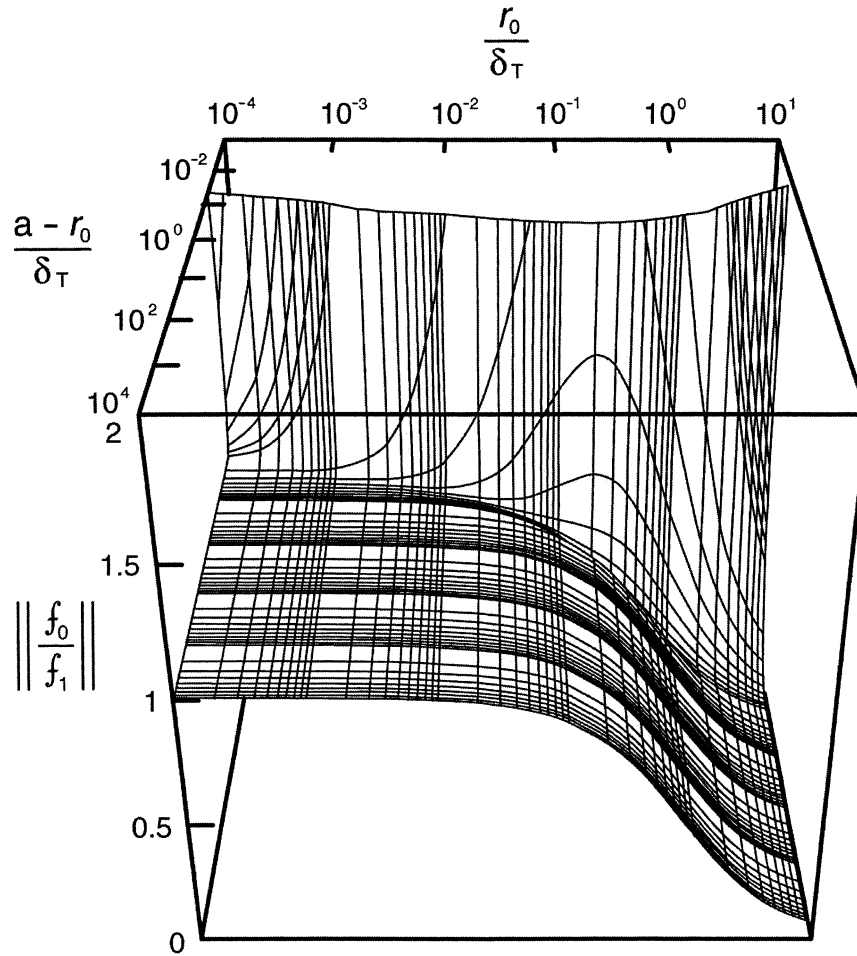


FIG. 1. Magnitude of $f_0(\lambda\eta_0, \lambda)/f_1(\lambda\eta_0, \lambda)$ vs the normalized particle radius and normalized neighborhood thickness $[(a - r_0)/\delta_T]$.

for $(a - r_0)/\delta > 1$. A significant variation in phase will occur for r_0/δ_T of a few tenths, significant magnitude changes for r_0/δ_T approaching one.

c. *Effect of thermal equilibration time of an isolated particle surrounded by gas*

Equation (55) express the effect of the thermal equilibration time of an isolated particle surrounded by a gas (Chan 1975; Marble 1969). Marble has derived the following expression for the thermal equilibration time:

$$\tau_T = \frac{c_{pp}\rho_p r_0^2}{3\kappa}. \tag{57}$$

Equation (54) can then be written as $Th = \tau_T\omega$, when $f_0(\lambda_T\eta_0, \lambda_T)/f_1(\lambda_T\eta_0, \lambda_T)$ and c' are one. For our more general analysis, we write this term out in terms of the particle radius normalized by the thermal penetration depth:

$$\begin{aligned} Th &= \frac{2}{3} \left(\frac{c_{pp}\rho_p}{c_p\rho} \right) \left(\frac{r_0}{\delta_{Tair}} \right)^2 \left(\frac{c'}{1 + (1 - i)r_0/\delta_T} \right) \\ &= \omega\tau_T \left[\frac{c'}{1 + (1 - i)r_0/\delta_T} \right]. \end{aligned} \tag{58}$$

We have utilized the large neighborhood from for the ratio of functions $f_0(\lambda_T\eta_0, \lambda_T)/f_1(\lambda_T\eta_0, \lambda_T)$. The ratio in square brackets is 120 for water drops in air. Equation (58) will be significant with respect to one for $r_0/\delta_T > 0.03$. At 1500 Hz this corresponds to particle radii greater than 2 μm ; at 20 kHz greater than 0.5 μm . By comparison, typical soot equivalent-volume-sphere radii in the atmosphere are typically below 0.5 μm .

6. **Approximate expressions for the source terms**

It is useful to rewrite the source terms in the simplified form that is correct for lower-particle densities but with arbitrary particle size:

$$h = \frac{c'}{\Xi}, \tag{59}$$

$$m = \frac{c'Ev}{\Xi}, \tag{60}$$

with

$$Ev = \frac{\rho_2^0 D_{12} \rho_0}{\kappa T_0 \rho_1^0} \left(\frac{lm_2}{RT_0} - 1 \right) \frac{1 + (1 - i)r_0/\delta_D}{1 + (1 - i)r_0/\delta_T}, \tag{61}$$

$$\Xi = 1 - iTh + lEv, \text{ and} \tag{62}$$

$$c' = 1 + i \frac{2}{15} \left(\frac{r_0}{\delta_{Tp}} \right)^2. \tag{63}$$

The thermal term Th is given in Eq. (58). These terms can be further simplified for $r_0/\delta_T < 0.1$ by eliminating the $(1 - i)r_0/\delta$ terms to form simplified equations. For the DRI instrument operated at 1500 Hz, this is valid for particles smaller than 6 microns.

7. Results

Figure 2 displays the predicted magnitude and phase of the ratio of acoustic pressure to the laser power as a function of normalized radius for a fog of water droplets. In this plot, the laser absorption in the fog is equal to the number density of drops times the laser absorption in a single drop. An absorption efficiency of $7.5 \text{ m}^2 \text{ g}^{-1}$ is used for the water droplet to simulate the light absorption by a carbonaceous particle, and obtain the absorption coefficient in dimensions of inverse distance by multiplying by the droplet mass concentration. The purpose of using explicit units is to evaluate the neighborhood effects for the DRI instrument, though it should be noted that the generated photoacoustic signals in this theory vary linearly with respect to the absorption efficiency. Such a large absorption efficiency for the water droplet would be relevant to use of IR sources, though for the purposes here, this detail is not needed. We assume the absorption efficiency per drop is constant and calculate the needed number density of drops for a given laser absorption in the fog and given drop size. Thus, for a laser absorption in the fog of 10 Mm^{-1} , the calculated number density at a normalized radius of $r_0/\delta_T = 10^{-3}$ is $1.2 \times 10^{-3} \text{ drops cm}^{-3}$ and $1.2 \times 10^{-3} \text{ drops cm}^{-3}$ for a normalized radius of $r_0/\delta_T = 1$.

Two effects can be observed in these figures: 1) for smaller particles, evaporation–condensation reduces the acoustic pressure relative to the energy absorbed, and 2) as the particles increase in size, thermal relaxation effects reduce the acoustic pressure in both wet and dry cases. The effect is largest for dry particles. Both of these dependences can be understood by examining the factor Ξ [Eq. (62)]. The inverse of this factor expresses the reduction in particle surface temperature for a given heat input relative to a dry particle small enough for thermal relaxation to be negligible. The thermal relax-

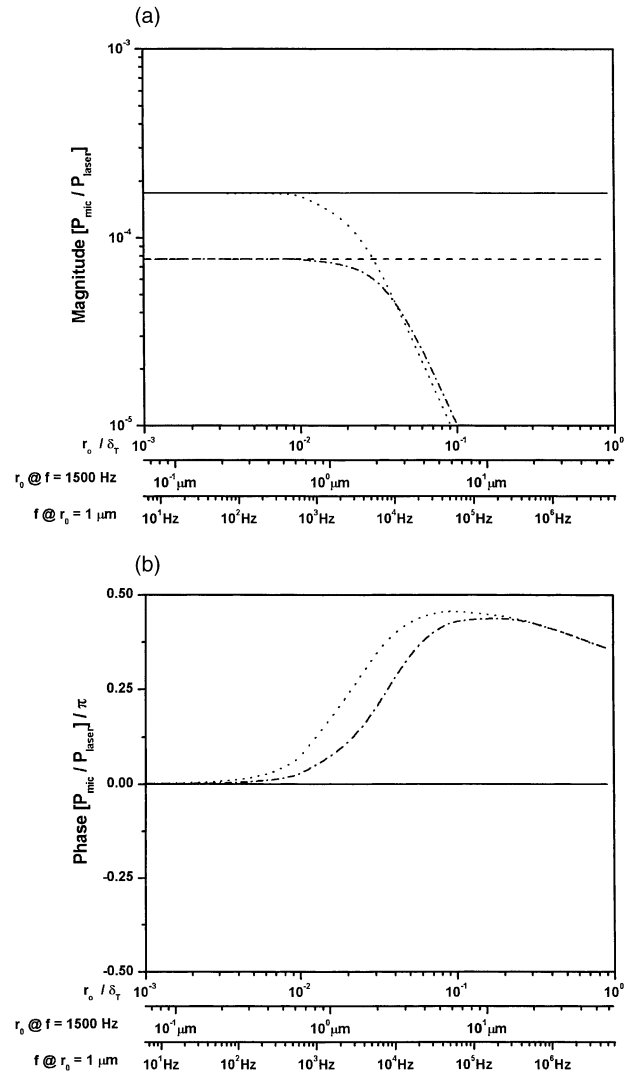


FIG. 2. (a) Magnitude and (b) phase of the microphone response for Baker's theory and Eq. (51) for $Babs = 10 \text{ Mm}^{-1}$. The ambient air pressure is 1 atm and the ambient temperature is 290 K. Solid line is for Baker's theory for dry particles and dashed line is for Baker's theory for wet particles. Dotted line is calculated using Eq. (51) for dry particles and the dot-dash line is calculated using Eq. (51) for wet particles. Dry particles are obtained simply by setting the mass diffusion coefficient to zero. First horizontal axis is for the ratio of particle radius and thermal penetration depth; the second axis displays actual particle radius for a resonator frequency of 1500 Hz; the third axis displays the dependence of acoustic pressure on frequency for a fixed particle radius.

ation term is a larger effect in reducing the temperature of a dry particle since the relaxation effects become large when Eq. (58) is $O(1)$ for a dry particle and $O(1 + lEv)$ for a wet particle.

For very large particles, the thermal term would dominate the factor Ξ and the ratio of wet to dry particle sound pressure ratios approaches $[1 + Ev c^2/(\gamma - 1)]$. At 20°C and 100% relative humidity with a particle size of $r_0/\delta_T = 0.1$, this factor is 1.24, in good agreement with Fig. 3.

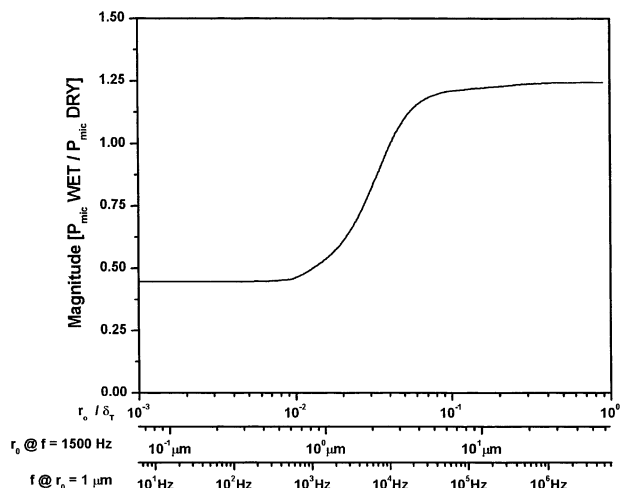


FIG. 3. Magnitude of the ratio of the microphone response of a wet particle to a dry particle for $Babs = 10 \text{ Mm}^{-1}$. The ambient air pressure is 1 atm and the ambient temperature is 290 K.

As the particle size approaches one thermal penetration depth the ratio of the terms $[1 + (1 - i)r_0/\delta_D]/[1 + (1 - i)r_0/\delta_T]$ slightly reduces the contribution of evaporation-condensation to the relative sound pressure level. We note that the sound pressure level for such conditions may not be detectable (see the far right portion of Fig. 2).

Additional horizontal axes are provided in Fig. 2 to aid interpretation. The second axis displays the actual particle radius for a resonator frequency of 1500 Hz. The third axis displays the dependence of the acoustic pressure on frequency for fixed particle radius. This scaling is only correct if particle neighborhood effects are negligible over the range of the plot. This display suggests that a multifrequency device could be used to investigate evaporation–condensation and thermal equilibrium effects in volatile aerosols of unknown size if the particles are large enough (the attenuation of sound waves in air places an upper limit on the acoustic frequencies used). The approximate equations presented in Eqs. (59)–(62) perfectly reproduce Fig. 2 demonstrating that neighborhood effects are negligible at the number densities used.

The results in Fig. 2 are relevant to the DRI instrument, and can be generalized to evaluate the fractional change in the photoacoustic signal when the aerosol is wet or dry. Figure 3 shows the ratio of the magnitude of the photoacoustic signal for a wet aerosol to that of a dry aerosol. For a broad frequency range, this ratio is 0.42. In other words, the measured photoacoustically generated pressure by an aqueous droplet is a factor of 0.42 smaller than that of an equivalent “dry” droplet. This sets a useful likely upper limit for the influence of mass transfer on photoacoustic measurements of aerosol light absorption. For soot, one can dry the aerosol before measuring its light absorption to obtain at least a standard measure of light absorption. However, the direct

measurement of aerosol light absorption as a function of relative humidity, especially high RH beyond 80%, remains elusive by the photoacoustic instrument, or any other method.

8. Conclusions

The analysis presented above demonstrates that neighborhood effects can be neglected for most atmospheric aerosols. Useful forms of the acoustic mass and heat source terms have been developed which account for thermal equilibration effects at higher frequencies and for larger particles. The frequency dependence of the magnitude and phase of the acoustic pressure may serve as a diagnostic of the relative contribution of thermal equilibration and mass transfer as volatile liquids are absorbed on aerosol particles.

The efficiency factor involved with assuming an aerosol is dry when it is actually moist is 0.42 for a temperature of 20°C. In practice, this factor could be set to 1 by drying the air stream below an RH of 65%. Future work will investigate the possibility of using photoacoustic measurements to measure the hydration state of black carbon by exploiting the contribution of mass transfer to the acoustic signal.

Acknowledgments. This work was supported by the Office of Naval Research under Grant N00014-99-1-0912, by the National Science Foundation under Grant ATM-9871192, and by the Applied Research Initiative of the State of Nevada. Comments from a critical read by Lee Harrison are appreciated.

REFERENCES

- Ackerman, A. S., O. B. Toon, D. E. Stevens, A. J. Heymsfield, V. Ramanathan, and E. J. Welton, 2000: reduction of tropical cloudiness by soot. *Science*, **288**, 1042–1047.
- Adams, K. M., L. I. Davis Jr., S. M. Japar, and D. R. Finley, 1990a: Real-time, in situ measurement of atmospheric optical absorption in the visible via photoacoustic spectroscopy—IV. Visibility degradation and aerosol optical properties in Los Angeles. *Atmos. Environ.*, **24A**, 605–610.
- , —, —, —, and R. A. Cary, 1990b: Measurement of atmospheric elemental carbon: Real-time data for Los Angeles during summer 1987. *Atmos. Environ.*, **24A**, 597–604.
- Andreae, M. O., 2001: The dark side of aerosols. *Nature*, **409**, 671–672.
- Arnott, W. P., H. Moosmüller, C. F. Rogers, T. Jin, and R. Bruch, 1999: Photoacoustic spectrometer for measuring light absorption by aerosols: Instrument description. *Atmos. Environ.*, **33**, 2845–2852.
- , —, and J. W. Walker, 2000: Nitrogen dioxide and kerosene-flame soot calibration of photoacoustic instruments for measurement of light absorption by aerosols. *Rev. Sci. Instrum.*, **71**, 4545–4552.
- Baker, M. B., 1976: Energy absorption by volatile atmospheric aerosol particles. *Atmos. Environ.*, **10**, 241–248.
- Brand, C., A. Winkler, P. Hess, A. Miklós, Z. Bozóki, and J. Sneider, 1995: Pulsed-laser excitation of acoustic modes in open high-Q photoacoustic resonators for trace gas monitoring: Results for C_2H_4 . *Appl. Opt.*, **34**, 3257–3266.
- Bruce, C. W., and R. G. Pinnick, 1977: In-situ measurements of

- aerosol absorption with a resonant cw laser spectrophone. *Appl. Opt.*, **16**, 1762–1765.
- Chan, C. H., 1975: Effective absorption for thermal blooming due to aerosols. *Appl. Phys. Lett.*, **26**, 628–629.
- Chughtai, A. R., N. J. Miller, D. M. Smith, and J. R. Pitts, 1999: Carbonaceous particle hydration III. *J. Atmos. Chem.*, **34**, 259–279.
- Faxvog, F. R., and D. M. Roessler, 1982: Mass concentration of diesel particle emissions from photoacoustic and opacity measurements. *Aerosol Sci. Technol.*, **1**, 225–234.
- Fiedler, M., and P. Hess, 1990: High precision study of chemical relaxation in the system $N_2O_4 = 2NO_2$ by photoacoustic resonance spectroscopy. *J. Chem. Phys.*, **93**, 8693–8702.
- Fiegel, R. P., P. B. Hays, and W. M. Wright, 1989: Photoacoustic technique for the measurement of absorption line profiles. *Appl. Opt.*, **28**, 1401–1408.
- Foot, J. S., 1979: Spectrophone measurements of the absorption of solar radiation by aerosol. *Quart. J. Roy. Meteor. Soc.*, **105**, 275–283.
- Fox, D. G., W. C. Malm, B. Mitchell, and R. W. Fisher, 1999: Where there's fire, there's smoke: Fine particulate and regional haze. *Environ. Manage.*, 15–24.
- Hansen, J., M. Sato, R. Ruedy, A. Lacis, and V. Oinas, 2000: Global warming in the twenty-first century: An alternative scenario. *Proc. Natl. Acad. Sci. USA*, **97**, 6.
- Harshbarger, W. R., and M. B. Robin, 1973: The opto-acoustic effect: Revival of an old technique for molecular spectroscopy. *Chem. Res.*, **6** (10), 329–334.
- Hickey, C. J., R. Raspet, W. V. Slaton, 2000: Effects of thermal diffusion on sound attenuation in evaporating and condensing gas-vapor mixtures in tubes. *J. Acoust. Soc. Amer.*, **107**, 1126–1130.
- Hirschfelder, J. V., C. Curtiss, and R. B. Bird, 1954: *Molecular Theory of Gases and Liquids*. Wiley.
- Horvath, H., 1993: Atmospheric light absorption—A review. *Atmos. Environ.*, **27A**, 293–317.
- , J. Gorraiz, T. Habenreich, and C. Johnson, 1983: On the influence of light absorption on visibility: Experimental laboratory study and measurement in Vienna. *J. Aerosol Sci.*, **14**, 357–361.
- Jacobson, M. Z., 2001: Strong radiative heating due to the mixing state of black carbon in atmospheric aerosols. *Nature*, **409**, 695–697.
- Landau, L. D., and E. M. Lifshitz, 1997: *Fluid Mechanics*. 2d ed. Butterworth-Heinemann, 539 pp.
- Lighty, J. S., J. M. Veranth, and A. F. Sarofim, 2000: Combustion aerosols: Factors governing their size and composition and implications to human health. *J. Air Waste Manage. Assoc.*, **50**, 1565–1618.
- Lohmann, U., and J. Feichter, 2001: Can the direct and semi-direct aerosol effect compete with the indirect effect on a global scale? *Geophys. Res. Lett.*, **28**, 159–161.
- Marble, F. E., 1969: Some gasdynamic problems in the flow of condensing vapors. *Astronaut. Acta*, **14**, 585–614.
- Miklos, A., and P. Hess, 2001: Application of acoustic resonators in photoacoustic trace gas analysis and metrology. *Rev. Sci. Instrum.*, **72**, 1937–1955.
- Moosmüller, H., W. P. Arnott, C. F. Rogers, J. C. Chow, C. A. Frazier, L. E. Sherman, and D. L. Dietrich, 1998: Photoacoustic and filter measurements related to aerosol light absorption during the Northern Front Range Air Quality Study (Colorado 1996/1997). *J. Geophys. Res.*, **103**, 28 149–28 157.
- , and Coauthors, 2001: Time resolved characterization of diesel particulate emissions. 2. Instruments for elemental and organic carbon measurements. *Environ. Sci. Technol.*, **35**, 1935–1942.
- Morse, P. M., and K. U. Ingard, 1986: *Theoretical Acoustics*. Princeton University Press, 927 pp.
- National Research Council, 1993: *Protecting Visibility in National Parks and Wilderness Areas*. National Academic Press, 316 pp.
- Petzold, A., and R. Niessner, 1992: In situ measurements on carbon aerosols with photoacoustic spectroscopy. *SPIE Int. Soc. Opt. Eng. Proc.*, **1716**, 510–516.
- , and —, 1995: Novel design of a resonant photoacoustic spectrophone for elemental carbon mass monitoring. *Appl. Phys. Lett.*, **66**, 1285–1287.
- Pierce, A. D., 1989: *Acoustics: An Introduction to its Physical Principles and Applications*. Acoustical Society of America.
- Raspet, R., C. J. Hickey, and J. M. Sabatier, 1999: The effect of evaporation–condensation on sound propagation in cylindrical tubes using the low reduced frequency approximation. *J. Acoust. Soc. Amer.*, **105**, 65–73.
- Reif, F., 1965: *Fundamentals of Statistical and Thermal Physics*. McGraw-Hill.
- Roessler, D. M., 1984: Photoacoustic insights on diesel exhaust particles. *Appl. Opt.*, **23**, 1148–1155.
- Rosenzweig, A., 1980: *Photoacoustics and Photoacoustic Spectroscopy*. Wiley.
- Sigrist, M. W., 1994: Air monitoring by laser photoacoustic spectroscopy. *Air Monitoring by Spectroscopic Techniques*, M. W. Sigrist, Ed., Wiley, 127–186.
- Terhune, R. W., and J. E. Anderson, 1977: Spectrophone measurements of the absorption of visible light by aerosols in the atmosphere. *Opt. Lett.*, **1** (2), 70–72.
- Truex, T. J., and J. E. Anderson, 1979: Mass monitoring of carbonaceous aerosol with a spectrophone. *Atmos. Environ.*, **13**, 507–509.